European Polymer Journal 220 (2024) 113495

Contents lists available at ScienceDirect

European Polymer Journal

journal homepage: www.elsevier.com/locate/europolj

Development and 4D printing of magneto-responsive PMMA/TPU/Fe_3O_4 nanocomposites with superior shape memory and toughness properties

Afshin Ahangari [a], Hossein Doostmohammadi [a], Majid Baniassadi [a], Mahdi Bodaghi [b,*], Mostafa Baghani [a,*]

[a] School of Mechanical Engineering, College of Engineering, University of Tehran, Tehran, Iran
[b] Department of Engineering, School of Science and Technology, Nottingham Trent University, Nottingham NG11 8NS, UK

ARTICLE INFO

Keywords:
Shape memory polymer
Nanocomposite
PMMA/TPU/Fe_3O_4
4D Printing
Remote magnetic actuation

ABSTRACT

This paper introduces 4D printing of composites of polymethyl methacrylate (PMMA) and thermoplastic polyurethane (TPU) reinforced with Fe_3O_4 particles for the first time. PMMA/TPU blends with 70/30 wt% are selected as matrix with the best compatibility based on dynamic mechanical thermal analysis. Fe_3O_4 nanoparticles are added to the blends with 10 %, 15 % and 20 % weight ratios. Their addition enables remote actuation of the materials in a high frequency alternating magnetic field. Field emission scanning microscopic images confirms a full dispersion of nanoparticles inside the polymeric matrix. Nanocomposites with 20 wt% of Fe_3O_4 can perfectly recover the permanent shape within 1.5 min in the magnetic field. They also reveal perfect shape memory properties in the hot water. Moreover, all samples display a perfect shape fixity ratio. The addition of TPU significantly enhances the toughness and flexibility of the PMMA matrix. It is found that Fe_3O_4 nanoparticles further enhance the mechanical strength by 10 % to 15 %, although they reduce the strain at break from 17 % to 14 %. Finally, a gripper is 4D printed and its excellent performance in the magnetic field is demonstrated.

1. Introduction

Shape memory polymers (SMPs) are a class of smart materials that can keep a temporary shape and recover their primary original shape when exposed to a suitable external stimulus such as heat, light, electric and magnetic fields [1–7]. The majority of SMPs are thermosensitive polymers [8–12]. The original shape is recovered when the temperature surpasses a certain threshold which is known as switching temperature (T_{switch}) [13,14]. Thermoplastic shape memory polymers consist of two distinct phases. In these structures, the domains with higher thermal transition temperature (T_{perm}) keep the permanent shape through their role as physical net points whereas secondary phase, exhibiting a different thermal transition temperature (T_{trans}) function as the trigger [15,16]. Above T_{trans}, the polymer chain segments of this phase become flexible which allows the material to exhibit significant elasticity. Below T_{trans}, movement of chains is restricted and therefore at this temperature the temporary shape of the polymer is fixed. In thermoplastic polymers, T_{trans} is typically the glass transition temperature (T_g) or the melting temperature (T_m).

In recent years, certain limitations within specific uses, as shown in Fig. 1, have drawn the academic interest towards the alternative methods of activating the shape memory polymers, predominantly through remote stimulation [17–21]. Magnetic shape memory polymers (MSMPs) are SMPs that can be remotely stimulated in a high-frequency alternating magnetic field, due to induction heating of superparamagnetic particles embedded within a thermosensitive SMP [21–29].

Researchers have utilized different materials such as NdFeB, Ni-Mn-Ga, nickel powder and chiefly iron (III) oxide (Fe_3O_4) as the main magnetic particles in magnetic shape memory nanocomposites [30–32]. In these nanocomposites, the majority have demonstrated that shape recovery rates in an alternating magnetic field are comparable to those with direct heat actuation. Yakacki et al. [20] investigated the influence of the proportion of Fe_3O_4 particles on the mechanical properties and shape recovery effect of MSMPs. They concluded that by increasing the weight percentage of the particles, the amount of induced heat that is caused by exposure to the magnetic field increases and also decreases T_g of the polymer matrix. Another important result is that the increase in the number of particles causes more brittleness of the material and the material cannot withstand large strains. Yu et al. [33] developed a

* Corresponding authors.
E-mail addresses: mahdi.bodaghi@ntu.ac.uk (M. Bodaghi), baghani@ut.ac.ir (M. Baghani).

https://doi.org/10.1016/j.eurpolymj.2024.113495
Received 15 June 2024; Received in revised form 11 August 2024; Accepted 6 October 2024
Available online 19 October 2024

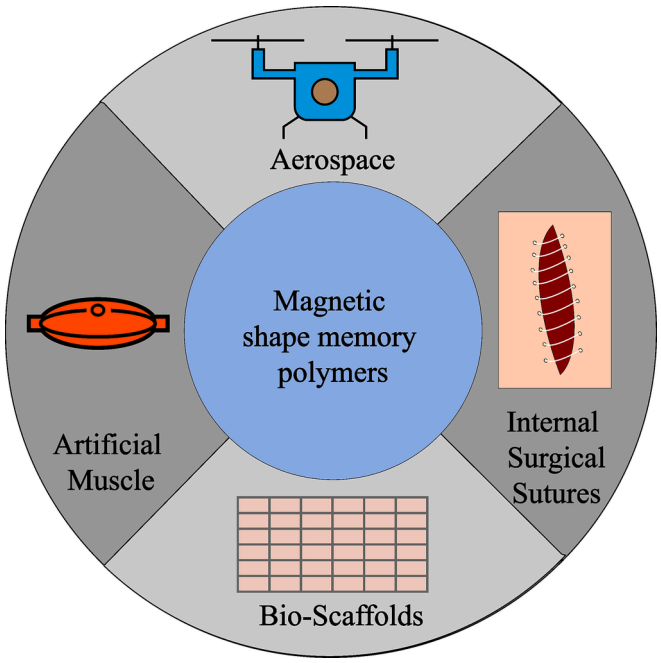

Fig. 1. MSMPs applications.

MSMP using poly(ε-caprolactone) (c-PCL) and Fe_3O_4 nanoparticles (5–25 % wt.). They found that crosslinking the polymer increased its shape recovery by up to 70 %. In their study, they compared the shape recovery rate in both direct heat (hot water) and an alternating magnetic field and observed that the shape recovery of c-PCL/Fe_3O_4 in hot water is much faster than in an AC magnetic field. Zhang et al. [34] created a MSMP using PLA with embedded Fe_3O_4 particles (15 % wt.) that can be activated by an AC magnetic field. They examined the shape memory properties of this material for potential use in biomedical applications. They discovered that a bone support structure they developed could rapidly return to its original shape in a few seconds when subjected to the magnetic field, with the surface temperature remaining uniform at around 40 °C, making it safe for use in the human body. They reported a shape recovery rate of approximately 96 %, with bones regaining their original shape within 100 s under the alternating magnetic field at 27.5 kHz. They also noted that the shape recovery time in hot water was much faster, at about 10 s.

Thermoplastic polymers exhibit shape memory effect when they are crystalline or blended with other polymers. In thermoplastic blends, the shape memory effect is attributed to the two-phase morphology of the materials. The rigid amorphous regions in the blends can act as substitutes for the hard segments found in thermoset polymers and entanglement and bonding between two different polymer chains can serve as a form of crosslinking, known as physical crosslinking.

Nowadays, the progress in additive manufacturing (AM) techniques have allowed fabrication of many complex shapes that were previously costly to create using traditional methods [35–38]. While AM offers numerous advantages, such as increased design flexibility and reduced lead times, material selection remains a critical factor due to limitations in the range of materials that can be effectively utilized in 3D printing processes. One approach to address this challenge is the blending of materials with 3D printable polymers, although this can alter the properties of the base polymer. As a result, researchers have focused on developing material blends that maintain the desired characteristics while being compatible with additive manufacturing processes. Some other researchers have modified the characteristics of one polymer by blending technique [39].

Poly methyl methacrylate (PMMA) is a lightweight material with good rigidity and transparency. It is used in many industries including automotive and biomedical applications [40]. However, PMMA has low toughness, making it difficult to use as a 3D printing material. To improve the mechanical properties, PMMA can be blended with other 3D printable materials that have good toughness. One such material is Thermoplastic Polyurethane (TPU). TPU is a great 3D printing candidate as it has high toughness and flexibility [39]. Combining TPU with PMMA can enhance the printability by reducing the brittleness of PMMA, resulting in less chain shrinkage during the printing process.

In previous study, PMMA was added to PLA matrix to enhance the mechanical robustness and shape memory properties of pure PLA [41]. In this study, the goal was to develop 4D printed PMMA/TPU/Fe_3O_4 nanocomposites for the first time to enhance the toughness and flexibility of PMMA and make a 3D printable material with superior remotely controlled shape memory properties. This research investigated the mechanical properties and shape memory behaviors of these materials, using both direct and remote heating actuations. By adding Fe_3O_4 nanoparticles, these materials can be remotely activated using a high-frequency alternating magnetic field.

First, to achieve the best combination of PMMA/TPU blends, dynamic mechanical thermal analysis (DMTA) tests were performed and the best combination was chosen for being blended with Fe_3O_4 nanoparticles and once again DMTA tests were carried out to check the effect of these nanoparticles on morphological and physical behavior of the blends. Then, field emission scanning electron microscopy (FE-SEM) was utilized to evaluate the dispersity of nanoparticles inside the polymeric matrix. Energy dispersive X-ray (EDX) mapping was also used to confirm the FE-SEM results. The shape memory tests were performed in both hot water (for direct actuation) and a high-frequency alternating current (for indirect actuation) with the frequency of f = 100 kHz. The mechanical tests were also performed with a universal testing machine to evaluate the mechanical behavior of the samples. Finally, these composite materials were proposed as mechanically robust grippers and consequently a 3D gripper was printed to successfully show the capabilities of the material in this type of application.

2. Materials and methods

2.1. Materials

Poly methyl methacrylate (PMMA) granules with density of 1.19 g/cm^3, melt flow rate of 1.8 g/10 min and thermoplastic polyurethane filament (eTPU-95A) with diameter of 1.75 mm, processing temperature of 210–240 °C were purchased from YOUSU (Guangzhou, China) and eSUN (Shenzhen, China) respectively and magnetite (Fe_3O_4) nanoparticles coated with polyvinylpyrrolidone (PVP) were purchased from US Research Nanomaterials, Inc. (Houston, Texas, USA). The spherical particles had a size of 20–30 nm, surface area of 40–60 m^2/g, bulk density of 0.84 g/cm^3 and true density of 4.8–5.1 g/cm^3.

2.2. Processing and 4D printing

A pelletizer machine was used to chop the TPU filament into granules. Then, the TPU and PMMA granules were placed in a vacuum-controlled oven at 85 °C for a duration of 8 h in order to eliminate moisture and unpolymerized monomers. For fabrication of PMMA/TPU blends TPU with 3 different weight ratios (10 %, 20 % and 30 %) were added to PMMA in THF solvent (20 gr/300 ml). The solution was stirred utilizing a mechanical stirrer for 5 h and then Fe_3O_4 nanoparticles (with 3 different weight ratios of 10 %, 15 % and 20 %) were added to the solution and the mixture was stirred for 3 h at the speed of 1200 rpm. The solution was casted onto a flat surface and after the sheets were prepared, they were sliced into small pieces to be fed to the pellet-based 3D printer (Chakad, CCS1). The whole process is described in Fig. 2.

The parameters listed in Table 1 are used for printing the samples required for the tensile test and shape recovery test. The nozzle temperature for PMMA/TPU/Fe_3O_4 specimens was higher than for PMMA/

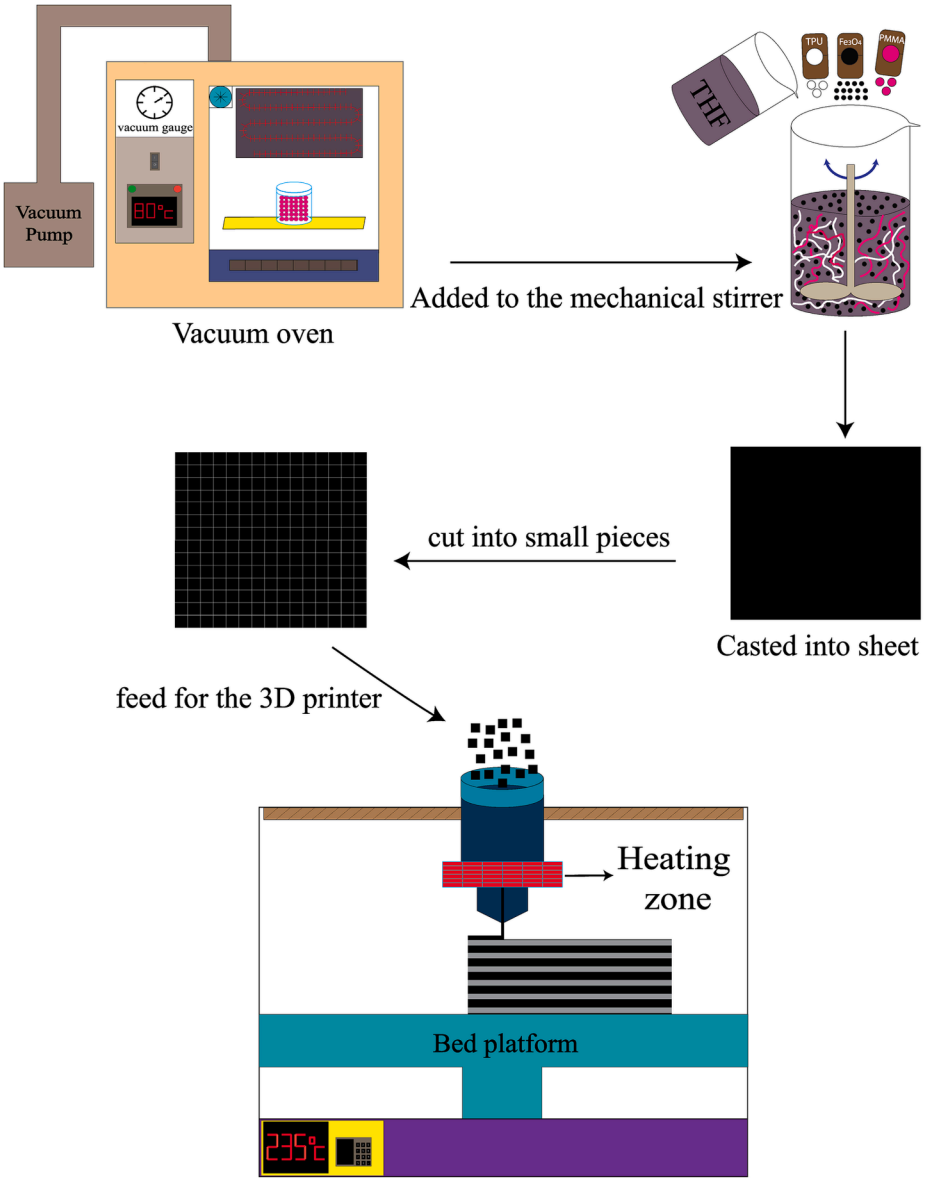

Fig. 2. The process of fabricating PMMA/TPU/Fe_3O_4 nanocomposites.

Table 1
3D printing parameters of samples.

Material	Nozzle Temperature (°C)	Bed Temperature (°C)	Printing Speed (mm/min)	Raster Angle (deg)
PMMA/TPU	210	40	400	0°/90°
PMMA/TPU/Fe_3O_4 (10 % wt.)	220	50	300	0°/90°
PMMA/TPU/Fe_3O_4 (15 % wt.)	220	50	300	0°/90°
PMMA/TPU/Fe_3O_4 (20 % wt.)	230	50	300	0°/90°

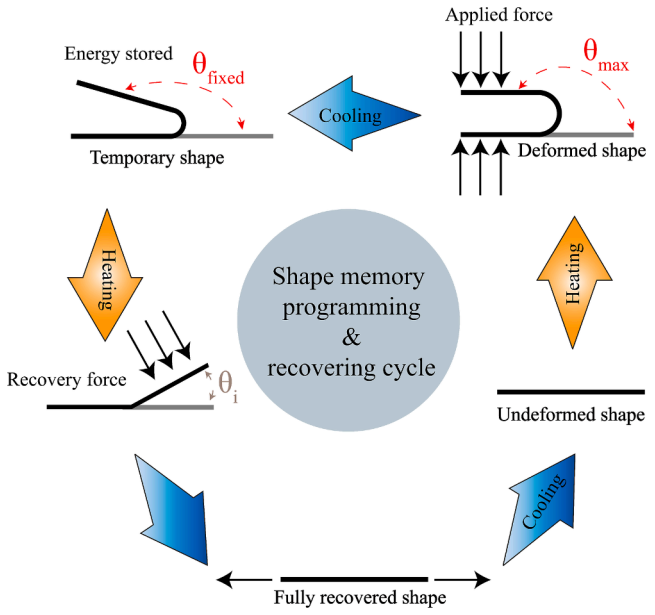

Fig. 3. Shape memory programming and recovering cycle in bending mode.

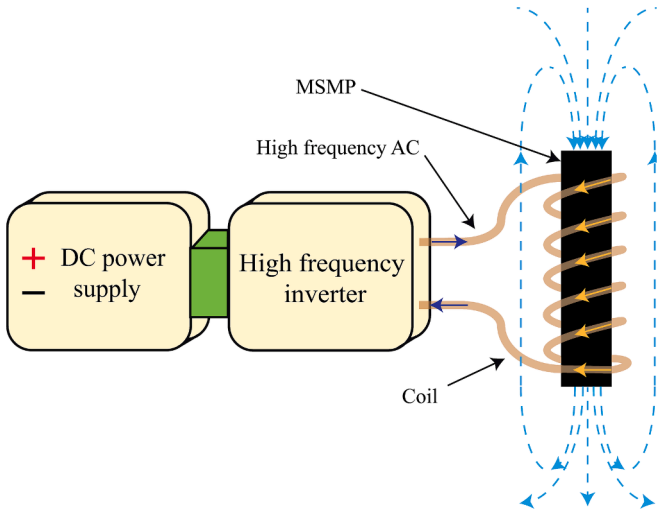

Fig. 4. Schematics of high frequency AC magnetic field and induction heating setup.

TPU because of the lower flowability of the material. Printing rate and bed temperature were carefully adjusted to minimize printing defects, such as poor layer adhesion and edge lifting off from the bed, with raster angles chosen based on the performance of samples in the shape recovery and tensile tests.

2.3. Characterization

DMTA was carried out with a dynamic mechanical analyzer from DMA 242C (NETZSCH, Germany), using tension mode at a heating rate of 5 °C/min and oscillation frequency of 1 Hz. All DMTA samples were 3D printed into rectangular shapes with dimension of 20 × 5 × 1 mm^3. T_g domain can be seen in storage modulus curves when there is a sharp decrease in the material's storage modulus (E').

Morphology of nanocomposites was analyzed using field emission scanning electron microscopy (FE-SEM) with a TESCAN MIRA 3 (TESCAN, Brno, Czech Republic). For this examination, rectangular samples measuring 10 × 10 × 1 mm^3 were 3D printed. Energy dispersive X-ray (EDX) mapping analysis was also conducted to determine the distribution of Fe_3O_4 on the surface of the samples. PMMA/TPU samples underwent chemical etching with chloroform solvent for 45 min to partially dissolve the PMMA phase (overexposure could result in sample failure).

2.4. Tensile test

Tensile tests were conducted to examine the mechanical properties of the nanocomposites using SANTAM STM-05. The samples were 3D printed following the ASTM D638 type V standard.

2.5. Shape memory behaviors

To investigate the shape memory behavior of nanocomposites in two states of actuation – direct heat and induction heat – the bending mode shown in Fig. 3 was used. In these two states, the shape recovery ratio (R_r) and the shape fixity ratio (R_f) were calculated according to Eqs. (1) and (2), respectively. θ_{max} represents the temporary angle applied to the samples under constraints ($T > T_g$), θ_{fixed} denotes the fixed angle once the constraints are removed ($T < T_g$), and θ_i signifies the residual angle post-exposure to stimuli ($T > T_g$).

$$R_f = \frac{\theta_{fixed}}{\theta_{max}} \times 100\% \quad (1)$$

$$R_r = \frac{\theta_{max} - \theta_i}{\theta_{max}} \times 100\% \quad (2)$$

To evaluate the shape recovery performance of nanocomposites under high-frequency alternating magnetic fields, a specialized setup (Fig. 4) was employed. This system can generate frequencies up to 150 kHz and deliver power outputs reaching 2 kW. For direct heating stimulation, samples were placed in hot water at 95 °C. For the programming step, samples were heated to 105 °C (higher than T_g) and bent into 'U' shapes. The samples were then cooled to room temperature as the last step.

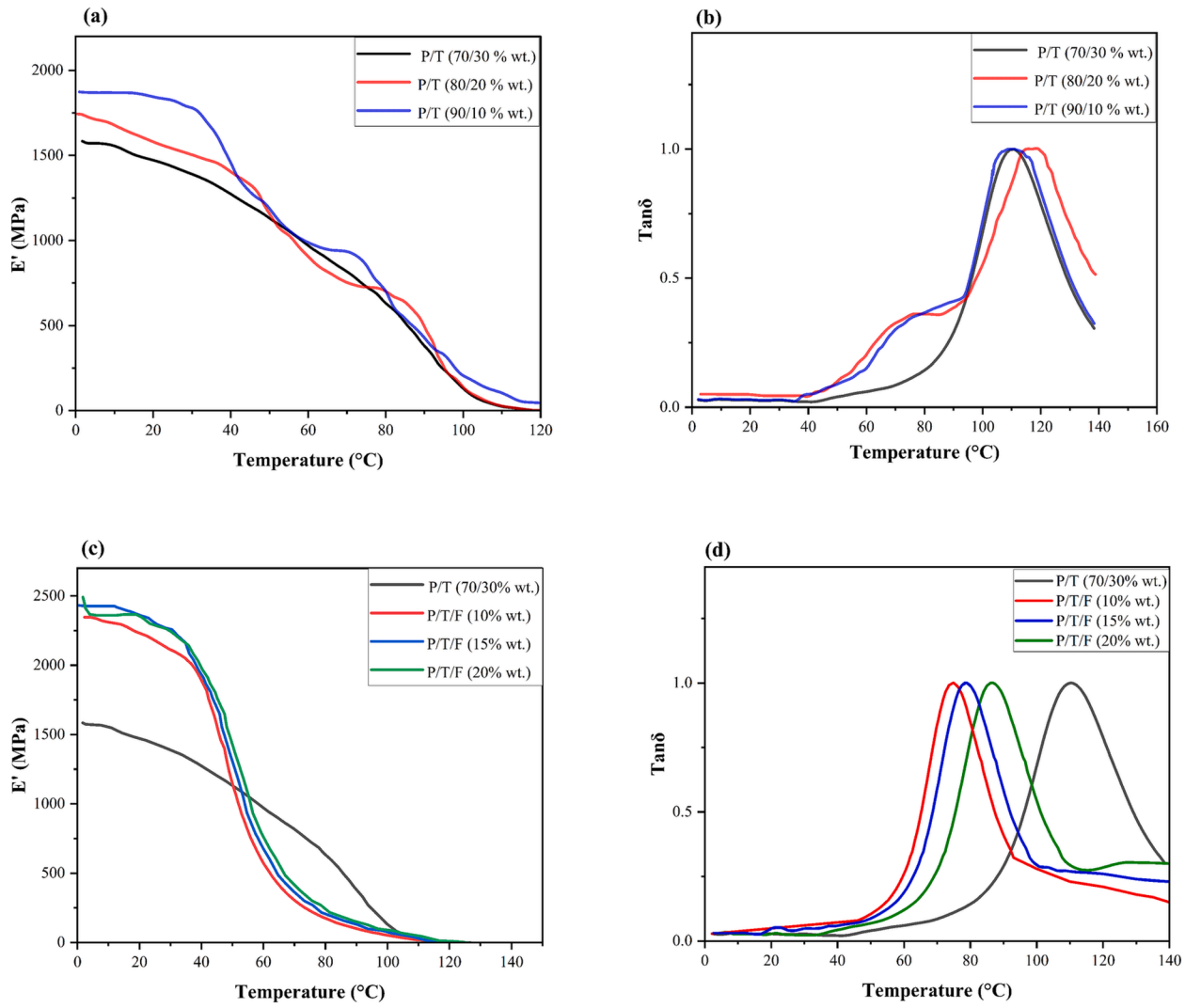

Fig. 5. DMTA results of (a, b) PMMA/TPU blends and (c, d) MSMPs.

Table 2
T_g of MSMPs.

Material	T_g (°C)
P/T (70/30 % wt.)	95
P/T/F (10 % wt.)	70.2
P/T/F (15 % wt.)	71.9
P/T/F (20 % wt.)	72.4

3. Results and Discussion

3.1. DMTA and thermal and dynamic mechanical properties

The DMTA results for all specimens are presented in Fig. 5. According to Fig. 5(a), blends with 30 % wt. of TPU shows a single transition temperature region which proves its compatibility with PMMA phase. Fig. 5(b) demonstrates tanδ of these blends which illustrates all PMMA/TPU blends have almost the same α-relaxation time according to the width of the peaks. This indicates that free volume in both materials is comparable and also the concentration of nanoparticles is small enough so that they do not form percolating networks and change the morphology of the polymer matrix. Fig. 5(c) shows that the addition of Fe_3O_4 affects the morphology and physical properties of these blends. First, it can be seen that storage modulus has increased dramatically by addition of magnetic nanoparticles, additionally, the thermal transition temperature of these structures has decreased drastically compared to its neat PMMA/TPU blends (depicted in Table 2). The increase in the storage modulus of the nanocomposites compared to PMMA/TPU blends is due to the high surface area of the magnetic nanoparticles, which interact strongly with the polymer chains. Restriction in chains mobility leads to stiffer material. Also, the steep loss in storage modulus of nanocomposites compared to PMMA/TPU blends can be an impact of both interfacial interaction of nanoparticles and superior heat transfer properties of nanoparticles. As mentioned in this section, stiffer regions in the material which are in the interface of nanoparticles and the polymer matrix soften much faster. Additionally, these nanoparticles have superior thermal conductivity and hence these regions are more rapidly heated. This shows that these materials can be actuated in environments like hot water. Unlike PMMA/TPU (70/30 % wt.), these blends have a narrower tanδ peak, which means that chains relax in a shorter time, MSMP with 20 % wt. of Fe_3O_4 has the lowest T_g compared to all other nanocomposites. The full list is provided in Table 2.

3.2. Morphology characterization

The morphological analysis of the MSMPs is provided in Fig. 6. As depicted in Fig. 6(a), TPU phases, which are etched by THF (with TPU having a much higher solution rate compared to PMMA) are fully

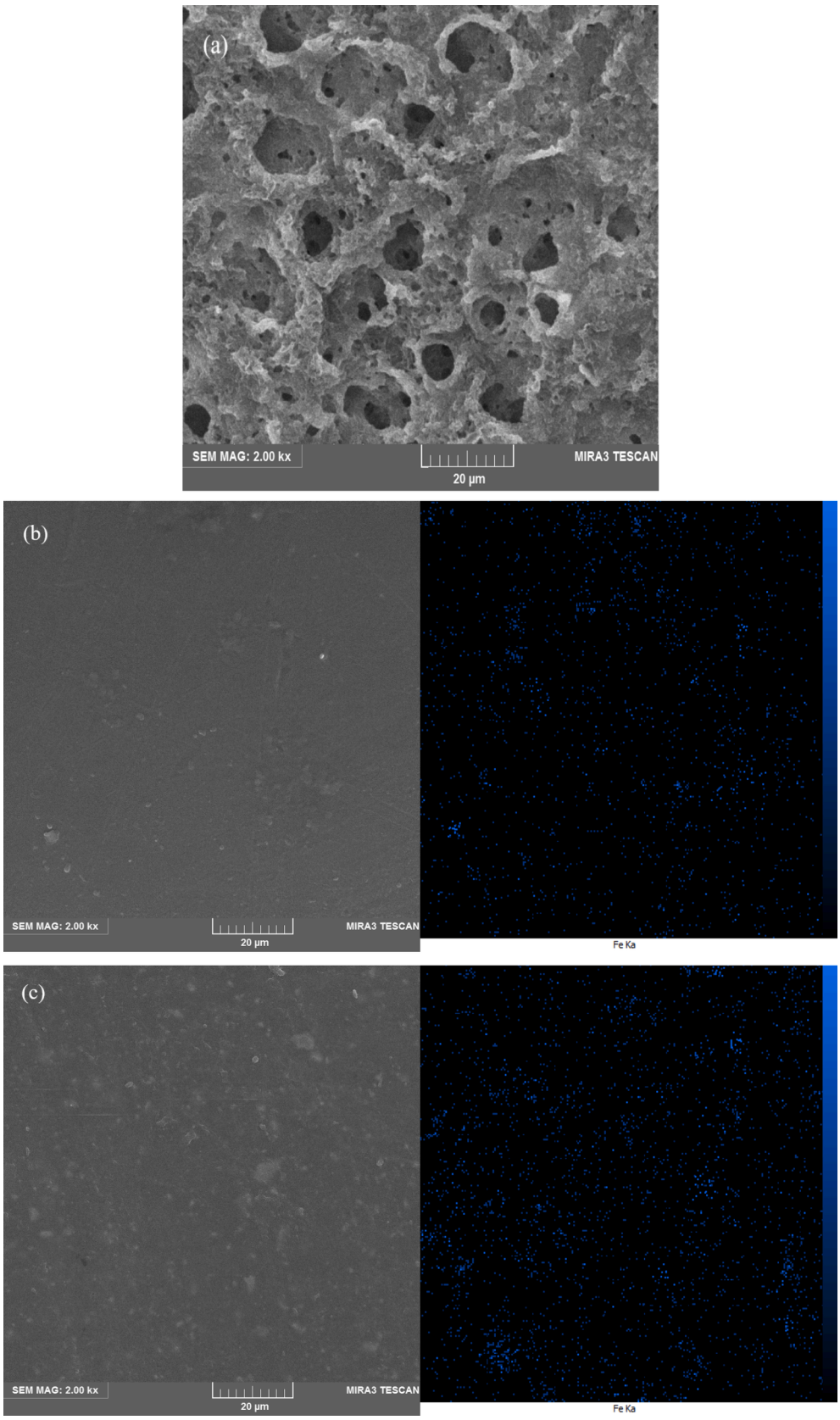

Fig. 6. (a) SEM image of chemically etched PMMA/TPU sample (b–d) SEM and EDX mapping images of PMMA/TPU/Fe_3O_4 samples with 10 %, 15 % and 20 % wt. of nanoparticles respectively.

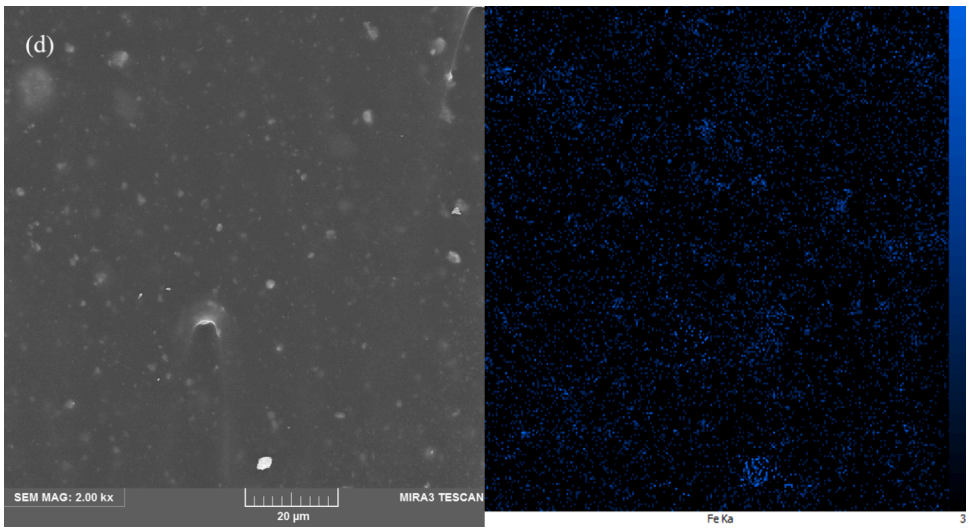

Fig. 6. (*continued*).

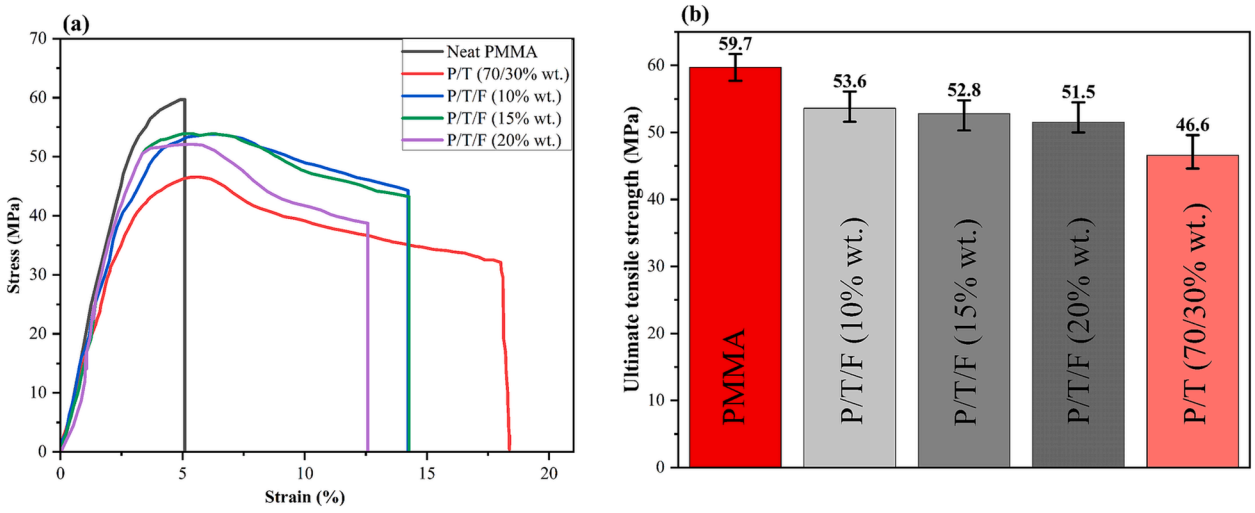

Fig. 7. (a) Stress-Strain curves and (b) UTS of MSMPs obtained from tensile test.

dispersed in the core–shell morphology of these blends. This full dispersion ensures uniform distribution of load in tensile test and also brings a uniform shape recovery in shape memory test. Fig. 6(b) to Fig. 6 (d) represent SEM and Fe element EDX mapping images of MSMPs with 10 %, 15 % and 20 % wt. of Fe_3O_4 respectively. In all these images, full dispersion is confirmed. Some agglomerated zones can be detected with diameters of less than 1 µm. These dispersed nanoparticles help better heat transfer when placed in magnetic field. These nanoparticles also can increase the temperature of the specimen when samples are actuated directly which results in faster shape recovery time compared to neat PMMA/TPU blends.

3.3. Mechanical properties

The stress–strain curves of the samples are displayed in Fig. 7. As illustrated, neat PMMA has an ultimate tensile strength (UTS) of 59.7 MPa with strain at break of 5 %. This rigidity was reduced by addition of 30 % wt. of TPU, which resulted in strain at break of 17 %. The recorded UTS is 46.5 MPa. In MSMPs, addition of Fe_3O_4 enhanced the mechanical strength of the nanocomposites. By increasing the amount of Fe_3O_4 content, the tensile strength increases. The strong interfacial bonding between polymer chains and nanoparticles is the reason behind this improvement. The enhanced interfacial area improves the mechanical interlocking and bonding, leading to increased strength. However, addition of nanoparticles more than 10 % wt. has led to creation of voids in 3D printing process and hence it resulted in a slight decrease in UTS of MSMPs. The Fe_3O_4 nanoparticles can obstruct the path of propagating cracks, causing them to deflect, branch, or even stop. This crack deflection mechanism toughens the material and enhances its resistance to fracture. However, the presence of Fe_3O_4 restricts the mobility of the chains and hence, the strain at break point is slightly decreased.

3.4. Shape memory properties

The results related to shape memory tests are presented in Fig. 8. It is worthy to discuss the shape fixing and shape recovery mechanisms first. In the shape changing process and at temperatures above T_g, PMMA chains and TPU's hard segments start to gain their mobility and the second shape can be fixed. TPU's soft domain provide the flexibility and the energy is stored in them. This stored energy acts as a driving force in shape recovery step. When the specimen is placed in magnetic field, the nanoparticles start to heat up and when their temperature reaches $T > T_g$, the heat is conducted through the specimen and all chains retain their permanent shape. Fig. 8(a) displays the shape changing

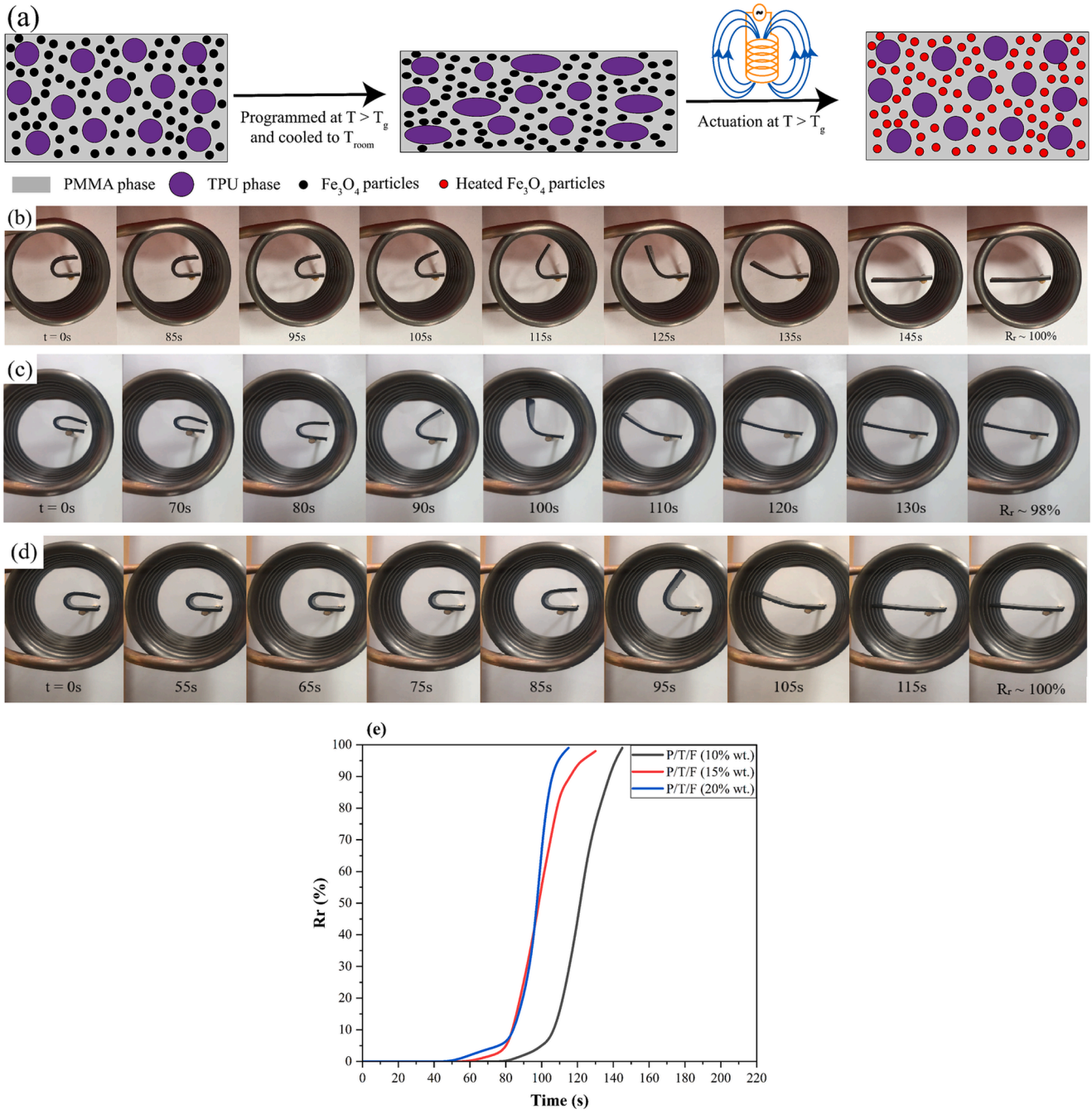

Fig. 8. (a) shape changing mechanism (b-d) shape recovery behavior of MSMPs with 10 %, 15 % and 20 % wt. of Fe_3O_4 (e) recovery ratio versus time for the three samples.

Table 3
Shape recovery properties of MSMPs (Induction actuation).

Material	R_f (%)	R_r (%)	Recovery time (s)	Magnetic field response time (s)
P/T/F (10 %)	100	100	145	82
P/T/F (15 %)	100	98	130	61
P/T/F (20 %)	100	100	115	45

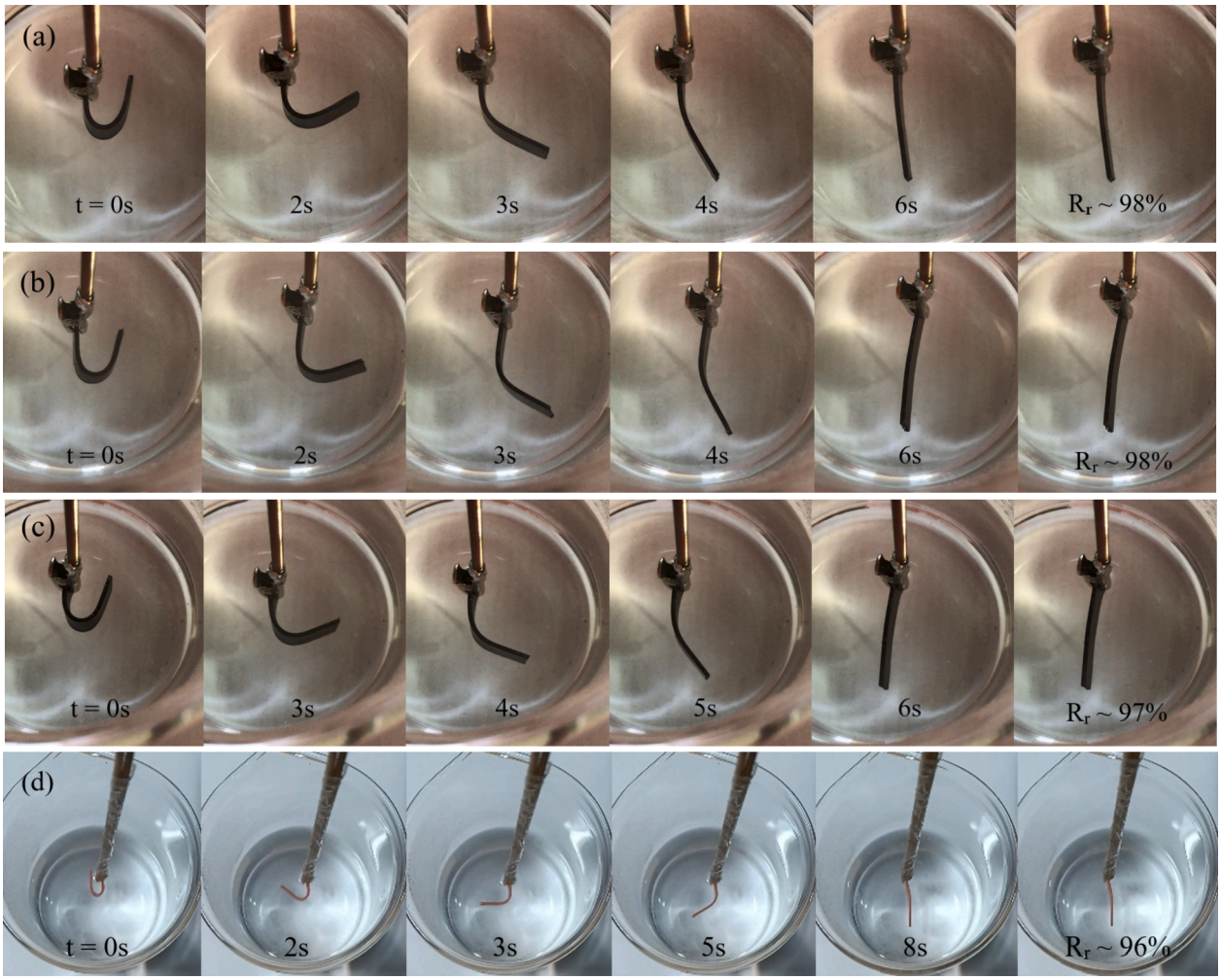

Fig. 9. Shape recovery behavior in direct actuation (a-c) MSMPs with 10 %, 15 % and 20 % wt. of Fe_3O_4 (d) PMMA/TPU.

Table 4
Shape recovery properties of MSMPs (Direct actuation).

Material	R_f (%)	R_r (%)	Recovery time (s)
P/T/F (10 %)	100	98	6
P/T/F (15 %)	100	98	6
P/T/F (20 %)	100	97	6
P/T	100	96	8

mechanism. Fig. 8(b–d) represents the behavior of MSMPs with 10 %, 15 % and 20 % wt. of nanoparticles in alternative magnetic field. As it can be seen, the higher content of magnetic nanoparticle, the faster the shape recovers and the higher the shape recovery ratio is. The samples have fully recovered and the recovery time for PMMA/TPU/Fe_3O_4 was less than two minutes (115 s) with perfect shape recovery ratio. Fig. 8(e) shows the recovery ratio versus time for the three samples. It also should be noted that all samples could record shape fixity ratio of 100 %.

Table 3 Illustrates the shape recovery properties of MSMPs. It also shows the magnetic response time of the specimens, which is the time taken by the specimen to respond to the magnetic field and the shape changing mechanism initiates.

For the direct heating actuation, Fig. 9, the samples were placed in hot water at 95 °C. The samples could perfectly recover their original shape within 6 s. The presence of nanoparticles accelerates the heating process in direct heating compared to neat PMMA/TPU. Table 4 indicates the shape recovery properties of MSMPs in hot water.

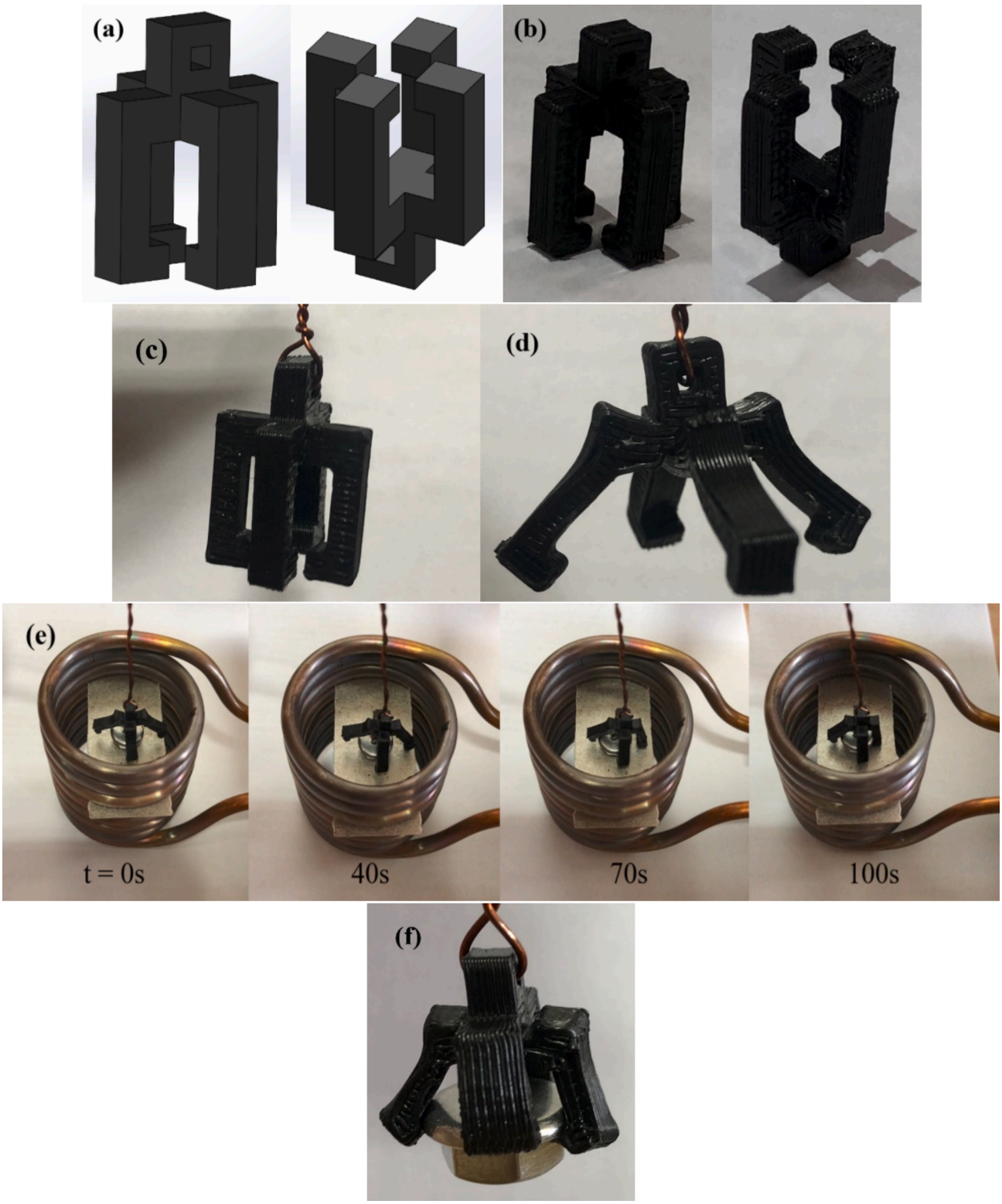

Fig. 10. (a) Designed gripper (b) 3D printed sample (c) original shape (d) temporary shape (e) gripper actuation under induction heating (f) final gripping shape.

4. 3D gripper as a potential application

Based on the developed MSMPs, and according to its mechanical and shape memory properties, it can be said that they are suitable for applications like grippers. The ultimate tensile strength of the PMMA/TPU/Fe_3O_4 blend provides good load-bearing capacity and resistance to tearing or deformation during gripping. This level of tensile strength helps ensure a secure and reliable grip on the target object.

The 12 % strain at break indicates that the PMMA/TPU/Fe_3O_4 blend has a moderate level of flexibility and elongation. This flexibility allows the gripper to conform to the shape of the object being gripped, improving the surface contact and overall grip performance.

The combination of PMMA and TPU in the blend can result in a material that is more durable and resistant to wear and tear compared to

pure PMMA or pure TPU. For better visualization, a 3D gripper has been 4D printed and its performance in magnetic field has been evaluated. According to Fig. 10, the sample could grip the target (aluminum specimen) in 100 s and recovered its permanent shape. The grip was tight and the gripper could successfully hold the specimen.

5. Conclusion

The current work focused on 4D printing of magneto-thermo responsive materials based on PMMA, TPU and Fe_3O_4 nanoparticles demonstrating enhanced toughness, flexibility, and shape memory. FE-SEM images along with DMTA assessed the compatibility of the blends and confirmed the core–shell morphology with great dispersity of TPU and Fe_3O_4 (10, 15 and 20 % wt.) phases in PMMA matrix in PMMA/TPU with 70/30 % wt. These materials were fabricated utilizing solution blending method. The processed sheets were cut into small pieces and fed into a pellet-based 3D printer. The prepared MSMPs were 4D printed for shape memory tests and tensile tests. The results showed shape recovery ratio of 100 % with UTS of 53.8 MPa for 10 % wt. of Fe_3O_4, ratio of 98 % with UTS of 52.8 for 15 %wt. of Fe_3O_4 and ratio of 100 % with UTS of 51.5 for 20 %wt. of Fe_3O_4. All samples showed perfect shape fixity (~100 %). Another important factor was the time performance of these nanocomposites in high frequency alternating magnetic field at which the best nanocomposite could recover its permanent shape within 1.5 min. The nanoparticles helped the specimen's heat faster and recover in shorter time compared to pure PMMA/TPU material. Finally, a gripper was 4D printed to show its capabilities of the materials in a high frequency AC magnetic field. The gripper could successfully hold and lift the object within 100 s. In this respect, this material can be proposed for potential use in gripper applications.

CRediT authorship contribution statement

Afshin Ahangari: Writing – original draft, Validation, Methodology, Investigation, Formal analysis, Data curation, Conceptualization. **Hossein Doostmohammadi:** Writing – review & editing, Software, Methodology, Investigation, Formal analysis, Data curation. **Majid Baniassadi:** Writing – review & editing, Supervision, Methodology, Investigation, Formal analysis. **Mahdi Bodaghi:** Writing – review & editing, Validation, Supervision, Software, Project administration, Methodology, Investigation, Formal analysis, Conceptualization. **Mostafa Baghani:** Writing – review & editing, Validation, Supervision, Project administration, Methodology, Investigation, Formal analysis.

Declaration of competing interest

The authors declare that they have no known competing financial interests or personal relationships that could have appeared to influence the work reported in this paper.

Data availability

Data are reported in research paper.

Acknowledgments

Mahdi Bodaghi acknowledges the support by the UK Engineering and Physical Sciences Research Council (EPSRC) (grant number EP/Y011457/1).

Appendix A. Supplementary material

Supplementary data to this article can be found online at https://doi.org/10.1016/j.eurpolymj.2024.113495.

References

[1] M. Behl, A. Lendlein, Shape-memory polymers, Mater. Today 10 (2007) 20–28, https://doi.org/10.1016/S1369-7021(07)70047-0.
[2] C. Liu, H. Qin, P.T. Mather, Review of progress in shape-memory polymers, J. Mater. Chem. 17 (2007) 1543, https://doi.org/10.1039/b615954k.
[3] C. Ni, D. Chen, Y. Yin, X. Wen, X. Chen, C. Yang, G. Chen, Z. Sun, J. Wen, Y. Jiao, C. Wang, N. Wang, X. Kong, S. Deng, Y. Shen, R. Xiao, X. Jin, J. Li, X. Kong, Q. Zhao, T. Xie, Shape memory polymer with programmable recovery onset, Nature 622 (2023) 748–753, https://doi.org/10.1038/s41586-023-06520-8.
[4] W. Zhao, C. Yue, L. Liu, Y. Liu, J. Leng, Research progress of shape memory polymer and 4D printing in biomedical application, Adv. Healthc. Mater. 12 (2023), https://doi.org/10.1002/adhm.202201975.
[5] H. Liu, F. Wang, W. Wu, X. Dong, L. Sang, 4D printing of mechanically robust PLA/TPU/Fe_3O_4 magneto-responsive shape memory polymers for smart structures, Compos. B Eng. 248 (2023) 110382, https://doi.org/10.1016/j.compositesb.2022.110382.
[6] H. Meng, G. Li, A review of stimuli-responsive shape memory polymer composites, Polymer (Guildf) 54 (2013) 2199–2221, https://doi.org/10.1016/j.polymer.2013.02.023.
[7] Y. Wang, Y. Wang, Q. Wei, J. Zhang, Light-responsive shape memory polymer composites, Eur. Polym. J. 173 (2022) 111314, https://doi.org/10.1016/j.eurpolymj.2022.111314.
[8] X. Huang, M. Panahi-Sarmad, K. Dong, Z. Cui, K. Zhang, O. Gelis Gonzalez, X. Xiao, 4D printed TPU/PLA/CNT wave structural composite with intelligent thermal-induced shape memory effect and synergistically enhanced mechanical properties, Compos. Part A Appl. Sci. Manuf. 158 (2022) 106946, https://doi.org/10.1016/j.compositesa.2022.106946.
[9] T. Yang, W. Chen, J. Hu, B. Zhao, G. Fang, F. Peng, Z. Cao, Thermal conduction behaviors of single-ply broken twill weave reinforced thermally induced resin-based shape memory polymer composites: multi-scale method analysis and laser flash analysis, Appl. Compos. Mater. 29 (2022) 473–496, https://doi.org/10.1007/s10443-021-09977-w.
[10] Y. Bai, L. Ionov, A thermo-, near-infrared light- and water-induced shape memory polymer with healing fatigued shape memory performance, Mater. Chem. Front. 6 (2022) 1218–1227, https://doi.org/10.1039/D2QM00041E.
[11] M. Mattmann, C. De Marco, F. Briatico, S. Tagliabue, A. Colusso, X. Chen, J. Lussi, C. Chautems, S. Pané, B. Nelson, Thermoset shape memory polymer variable stiffness 4D robotic catheters, Adv. Sci. 9 (2022), https://doi.org/10.1002/advs.202103277.
[12] B.G. Molina, G. Ocón, F.M. Silva, J.I. Iribarren, E. Armelin, C. Alemán, Thermally-induced shape memory behavior of polylactic acid/polycaprolactone blends, Eur. Polym. J. 196 (2023) 112230, https://doi.org/10.1016/j.eurpolymj.2023.112230.
[13] T. Chatterjee, K. Naskar, Thermo-sensitive shape memory polymer nanocomposite based on polyhedral oligomeric silsesquioxane (POSS) filled polyolefins, Polym.-Plastics Technol. Mater. 58 (2019) 630–640, https://doi.org/10.1080/03602559.2018.1493127.
[14] A. Enferadi, M. Baniassadi, M. Baghani, Innovative multiphysics approach for designing high-performance thermo-responsive shape memory polymer microvalve, Eur. J. Mech. A. Solids 103 (2024) 105174, https://doi.org/10.1016/j.euromechsol.2023.105174.
[15] Y. Wang, Y. Wang, Q. Wei, J. Zhang, M. Lei, M. Li, D. Li, Effects of the composition ratio on the properties of PCL/PLA blends: a kind of thermo-sensitive shape memory polymer composites, J. Polym. Res. 28 (2021) 451, https://doi.org/10.1007/s10965-021-02815-4.
[16] Y. Xia, Y. He, F. Zhang, Y. Liu, J. Leng, A review of shape memory polymers and composites: mechanisms, materials, and applications, Adv. Mater. 33 (2021), https://doi.org/10.1002/adma.202000713.
[17] J. Xue, Y. Ge, Z. Liu, Z. Liu, J. Jiang, G. Li, Photoprogrammable moisture-responsive actuation of a shape memory polymer film, ACS Appl. Mater. Interf. 14 (2022) 10836–10843, https://doi.org/10.1021/acsami.1c24018.
[18] T. Li, J. Sun, J. Leng, Y. Liu, An electrical heating shape memory polymer composite incorporated with conductive elastic fabric, J. Compos. Mater. 56 (2022) 1725–1736, https://doi.org/10.1177/00219983221085630.
[19] A.U. Vakil, M. Ramezani, M.B.B. Monroe, Magnetically actuated shape memory polymers for on-demand drug delivery, Materials 15 (2022) 7279, https://doi.org/10.3390/ma15207279.
[20] C.M. Yakacki, N.S. Satarkar, K. Gall, R. Likos, J.Z. Hilt, Shape-memory polymer networks with fe 3O 4 nanoparticles for remote activation, J. Appl. Polym. Sci. 112 (2009) 3166–3176, https://doi.org/10.1002/app.29845.
[21] A.M. Schmidt, Electromagnetic activation of shape memory polymer networks containing magnetic nanoparticles, Macromol. Rapid Commun. 27 (2006) 1168–1172, https://doi.org/10.1002/marc.200600225.
[22] S.J.M. van Vilsteren, H. Yarmand, S. Ghodrat, Review of magnetic shape memory polymers and magnetic soft materials, Magnetochemistry 7 (2021) 123, https://doi.org/10.3390/magnetochemistry7090123.
[23] S. Huang, M. Shan, H. Zhang, J. Sheng, J. Zhou, C. Cui, J. Wei, W. Zhu, J. Lu, 4D printing of soybean oil based shape memory polymer and its magnetic-sensitive composite via digital light processing, Poly.-Plastics Technol. Mater. 61 (2022) 923–936, https://doi.org/10.1080/25740881.2022.2029891.
[24] U.N. Kumar, K. Kratz, W. Wagermaier, M. Behl, A. Lendlein, Non-contact actuation of triple-shape effect in multiphase polymer network nanocomposites in alternating magnetic field, J. Mater. Chem. 20 (2010) 3404–3415, https://doi.org/10.1039/b923000a.

[25] M.Y. Razzaq, M. Anhalt, L. Frormann, B. Weidenfeller, Thermal, electrical and magnetic studies of magnetite filled polyurethane shape memory polymers, Mater. Sci. Eng. A 444 (2007) 227–235, https://doi.org/10.1016/j.msea.2006.08.083.
[26] Y. Cai, J. Sen Jiang, B. Zheng, M.R. Xie, Synthesis and properties of magnetic sensitive shape memory Fe_3O_4/poly(ε-caprolactone)-polyurethane nanocomposites, J. Appl. Polym. Sci. 127 (2013) 49–56, https://doi.org/10.1002/app.36849.
[27] F. Zhang, L. Wang, Z. Zheng, Y. Liu, J. Leng, Magnetic programming of 4D printed shape memory composite structures, Compos. A Appl. Sci. Manuf. 125 (2019) 105571, https://doi.org/10.1016/j.compositesa.2019.105571.
[28] T. Weigel, R. Mohr, A. Lendlein, Investigation of parameters to achieve temperatures required to initiate the shape-memory effect of magnetic nanocomposites by inductive heating, Smart Mater. Struct. 18 (2009) 025011, https://doi.org/10.1088/0964-1726/18/2/025011.
[29] D. Yang, W. Huang, X. He, M. Xie, Electromagnetic activation of a shape memory copolymer matrix incorporating ferromagnetic nanoparticles, Polym. Int. 61 (2012) 38–42, https://doi.org/10.1002/pi.3188.
[30] R.U. Hassan, S. Jo, J. Seok, Fabrication of a functionally graded and magnetically responsive shape memory polymer using a 3 <scp>D</scp> printing technique and its characterization, J. Appl. Polym. Sci. 135 (2018), https://doi.org/10.1002/app.45997.
[31] P.R. Buckley, G.H. McKinley, T.S. Wilson, W. Small, W.J. Benett, J.P. Bearinger, M. W. McElfresh, D.J. Maitland, Inductively heated shape memory polymer for the magnetic actuation of medical devices, IEEE Trans. Biomed. Eng. 53 (2006) 2075–2083, https://doi.org/10.1109/TBME.2006.877113.
[32] I. Aaltio, F. Nilsén, J. Lehtonen, Y.L. Ge, S. Spoljaric, J. Seppälä, S.P. Hannula, Magnetic shape memory - polymer hybrids, Mater. Sci. Forum 879 (2016) 133–138, https://doi.org/10.4028/www.scientific.net/MSF.879.133.
[33] X. Yu, S. Zhou, X. Zheng, T. Guo, Y. Xiao, B. Song, A biodegradable shape-memory nanocomposite with excellent magnetism sensitivity, Nanotechnology 20 (2009), https://doi.org/10.1088/0957-4484/20/23/235702.
[34] X. Zhang, X. Lu, Z. Wang, J. Wang, Z. Sun, Biodegradable shape memory nanocomposites with thermal and magnetic field responsiveness, J. Biomater. Sci. Polym. Ed. 24 (2013) 1057–1070, https://doi.org/10.1080/09205063.2012.735098.
[35] M.Y. Khalid, Z.U. Arif, R. Noroozi, A. Zolfagharian, M. Bodaghi, 4D printing of shape memory polymer composites: A review on fabrication techniques, applications, and future perspectives, J. Manuf. Process. 81 (2022) 759–797, https://doi.org/10.1016/j.jmapro.2022.07.035.
[36] C.A. Spiegel, M. Hackner, V.P. Bothe, J.P. Spatz, E. Blasco, 4D printing of shape memory polymers: from macro to micro, Adv. Funct. Mater. 32 (2022), https://doi.org/10.1002/adfm.202110580.
[37] Y.S. Alshebly, M. Nafea, M.S. Mohamed Ali, H.A.F. Almurib, Review on recent advances in 4D printing of shape memory polymers, Eur Polym J 159 (2021) 110708, https://doi.org/10.1016/j.eurpolymj.2021.110708.
[38] A.A. Ameen, A.M. Takhakh, A. Abdal-hay, An overview of the latest research on the impact of 3D printing parameters on shape memory polymers, Eur. Polym. J. 194 (2023) 112145, https://doi.org/10.1016/j.eurpolymj.2023.112145.
[39] A. Zolfagharian, M. Denk, M. Bodaghi, A.Z. Kouzani, A. Kaynak, Topology-optimized 4D printing of a soft actuator, Acta Mech. Solida Sin. 33 (2020) 418–430, https://doi.org/10.1007/s10338-019-00137-z.
[40] X. Li, T. Liu, Y. Wang, Y. Pan, Z. Zheng, X. Ding, Y. Peng, Shape memory behavior and mechanism of poly(methyl methacrylate) polymer networks in the presence of star poly(ethylene glycol), RSC Adv. 4 (2014) 19273, https://doi.org/10.1039/c4ra01635a.
[41] H. Doostmohammadi, M. Baniassadi, M. Bodaghi, M. Baghani, 4D Printing of magneto-thermo-responsive PLA/PMMA/Fe_3O_4 nanocomposites with superior shape memory and remote actuation, Macromol. Mater. Eng. (2024), https://doi.org/10.1002/mame.202400090.